ACS OMEGA

http://pubs.acs.org/journal/acsodf

Article

Effect of Graphite on the Mechanical and Petrophysical Properties of Class G Oil Well Cement

Muhammad Andiva Pratama, Ahmed Abdulhamid Mahmoud, and Salaheldin Elkatatny*

Cite This: *ACS Omega* 2023, 8, 8773−8778

Read Online

ACCESS | Metrics & More | Article Recommendations

ABSTRACT: Casing cementing is one of the most crucial operations in the oil well drilling process since it determines the durability and stability of the well throughout its life. Different additives have been mixed into the oil well cement slurry to improve the properties of both the cement slurry and the solidified cement sheath. Graphite is a waste material with a huge potential to be utilized in cementing to improve the properties of the oil well cement and reduce the graphite waste content in the environment. This study intends to analyze the effect of graphite on alteration in properties of the cement compressive and tensile strength, Poisson's ratio, Young's modulus, porosity, and permeability for three days of curing. Based on the trend of the properties during the three days of curing, equations were established to describe the future change in cement properties with time. Two formulas of cement, the base (with no graphite) and graphite-based (with 0.2% by weight of cement graphite) were prepared in this study. The results showed that the graphite successfully increased the compressive strength, tensile strength, and Poisson's ratio of the cement sheath, throughout the curing process. Young's modulus was decreased after the incorporation of graphite which indicates an enhancement in cement resistance to shear forces. The porosity and permeability were also decreased indicating formation of a more densified cement sheath.

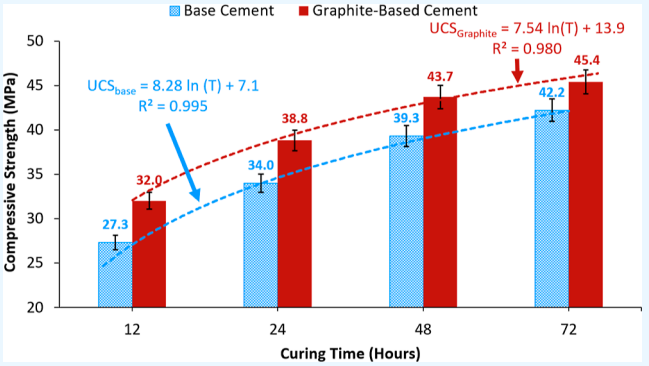

1. INTRODUCTION

Oil well cementing is a critical operation performed to achieve different functions to enable keeping the well steady and preventing leak of the formation fluid.[1] Therefore, different additives should be added to the cement slurry to enhance its properties. However, making an ideal drilling cement slurry is highly expensive with the materials present in the industry right now.[2] Extensive research was performed by different authors to find the most effective and efficient materials to be incorporated into the cement slurry to improve its properties.

The environmental issue must be considered while making the design of the various operations in the oil industry. Cementing operation is not an exception; finding "green" additives and process that provides high-quality cement is one thing that needs more consideration and investigation.[3−8]

The expected downhole condition is another important factor to be considered while designing the cement slurry formulation; this includes the expected pressure, temperature, fluids to contact the cement throughout the well lift, and so forth. This is because these conditions could significantly affect cement stability. For example, the high temperature and pressure could significantly deteriorate the long-term strength of the cement, which is leaking and affecting the stability of the well and probably will collapse.[9,10]

According to Dusseault et al.,[11] cement shrinkage could lead to leakage; cement shrinkage could happen when the cement is placed in a formation with high water and/or salt content.[12] Strength, rigidity, and bond are a function of time. Although it will rise as the curing time rises, it may also fall with further production time.[13]

Several researchers tried to improve the stability of cement in these difficult conditions by incorporating new additives,[14] to resist the high-pressure conditions,[15] improve the physical properties of the cement,[16] enhance the cement strength and rheology,[17] enhance the cement hydration and mechanical properties,[18] and to improve the properties of the high-density cement.[19]

Graphite is one of the minerals that occur in nature as a metamorphic rock. It formed as the result of the sedimentary process and is believed to have a stronger chemical bond than the diamond. The main composition of graphite is carbon (C).

Received: December 29, 2022
Accepted: February 10, 2023
Published: February 21, 2023

https://doi.org/10.1021/acsomega.2c08253
ACS Omega 2023, 8, 8773−8778

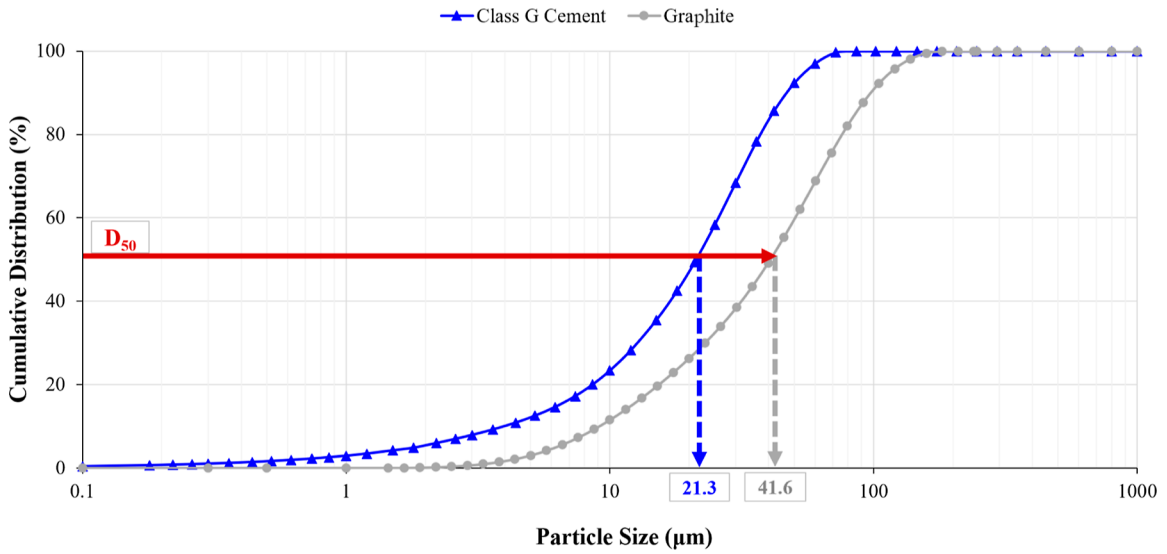

Figure 1. Particle size distribution of Saudi Class G cement and graphite powder.

Table 1. Mineral Composition of Saudi Class G Cement and Graphite

materials	Na	Mg	Al	Si	S	Cl	K	Ca	C	Ti	Mn	Fe	Zn	Sr
Class G	0	1.33	2.37	12.1	2.43	0	0	72.1	0	0.39	0.05	9.08	0	0.15
graphite	1.26	0.21	0.39	4.86	0.15	0.61	0.24	1.11	90.4	0.15	0.17	0.26	0.13	0.06

In industry, graphite usually appears as an environmentally hazardous waste.[20,21] Several studies were held to analyze the effect of additional graphite in the cement. Cai et al.[22] found that the addition of graphite improved the strength and deformation resistance of the common Class G cement. Mahmoud et al.[23] showed that the addition of the graphite could improve the carbonation resistance of Class G cement in CO_2 saturated environment.

The hydration reaction of the cement slurry plays an important role in the changes in cement properties, especially during the early time of hydration (i.e., cement curing). The time to wait on cement could considerably be affected by the rate of the cement properties variation, and this is directly affecting the cost of the drilling process.[24−26]

This study aims to evaluate the effect of the addition of graphite on the properties of the oil-well cement sheath of compressive strength, tensile strength, Poisson's ratio, and Young's modulus, porosity, and permeability; these properties will be evaluated with curing time. The sample will be hardened under the same conditions of temperature and pressure for varying times.

2. MATERIALS AND METHODOLOGY

2.1. Materials. In this study, two cement slurries were prepared using Saudi Class G cement; both slurries were prepared with a liquid-to-solid ratio of 0.44. The cement slurries also contain 0.8 %BWOC of dispersant and 0.7 % BWOC fluid loss controller. The slurries are different in graphite content, where the base slurry (the first formulation) has no graphite, and the graphite-based slurry (the second formulation) is prepared with 0.2 %BWOC graphite. The graphite content considered for the second formulation was based on the recommendation of Mahmoud et al.[23]

The particle size distributions for Saudi Class G cement and graphite powder are shown in Figure 1. The D_{50} for Class G cement is 21.3 μm, while for graphite is 41.6 μm. Table 1 compares the mineralogical composition of Class G cement and graphite as obtained by the X-ray fluorescence (XRF) characterization. As shown in this table, the majority of mineral that builds Class G cement is Calcium, while for graphite, the majority of mineral is carbon (more than 90%).

2.2. Experimental Methods. In this study, the mechanical properties of compressive and tensile strength, Young's modulus, and Poisson's ratio, in addition to the petrophysical properties of porosity and permeability of the two cement formulations under study were evaluated. After preparing the cement slurries of the two formulations under study according to the composition discussed earlier, the slurries were poured into metallic molds to prepare cement samples of different dimensions based on the test's specifications. The samples were cured at 90 °C and atmospheric pressure for 12, 24, 48, and 72 h before testing for the different properties.

2.2.1. Compressive Strength Measurement. For the compressive strength testing, cylindrical samples with 1.5 in. in diameter and 3.0 in. in length were prepared, and the compressive strength of the samples was measured using the scratch test. During the measurement, eight cuts were made in every sample, each cut with a depth of 0.05 mm. The measurement was repeated on three samples of every specimen; then the average of the three measurements was considered as the compressive strength of that sample.

2.2.2. Tensile Strength Measurement. For tensile strength testing, cylindrical samples with 1.5 in. in diameter and 0.9 in. in length were considered. The samples were tested following the Brazilian test procedure as explained by Mahmoud and Elkatatny.[27] While testing, the force was applied continuously along the circumference of the sample (at two opposite points) at a rate of 1.5 KN/s.

2.2.3. Elastic Property Measurement. The cement elastic properties of Poisson's ratio and Young's modulus were evaluated using samples with 1.5 in. in diameter and 3.0 in. in length. The elastic properties were determined based on the

https://doi.org/10.1021/acsomega.2c08253
ACS Omega 2023, 8, 8773−8778

ultrasonic velocity measurement which was conducted using the sonic mode of the scratch test machine.

2.2.4. Porosity and Permeability Measurement. The cement porosity was measured using the porosimeter, and the measuring fluid was helium. However, the permeameter was considered for permeability measurement, and the measuring fluid was nitrogen. Samples of 1.5 in. in diameter and 0.9 in. in length were considered for both porosity and permeability measurements.

3. RESULTS AND DISCUSSION

3.1. Compressive and Tensile Strength. The results of compressive and tensile strength measurements are shown in Figure 2 and Figure 3, respectively. As shown in Figure 2a, the compressive strength for both cement slurry systems increases with curing time, and the graphite-based samples have higher compressive strength at all curing times. After 12 h of curing, the addition of graphite into the cement slurry increased the compressive strength of the cement to 32 MPa compared to 27.3 MPa for the base sample. The compressive strength for both systems then increased with curing and tend to stabilize at 42.2 and 45.4 MPa for the base and graphite-based samples, respectively. This result proved that graphite has a positive impact not just on the durability of the cement, but the graphite can shorten the time needed to reach the desired compressive strength.

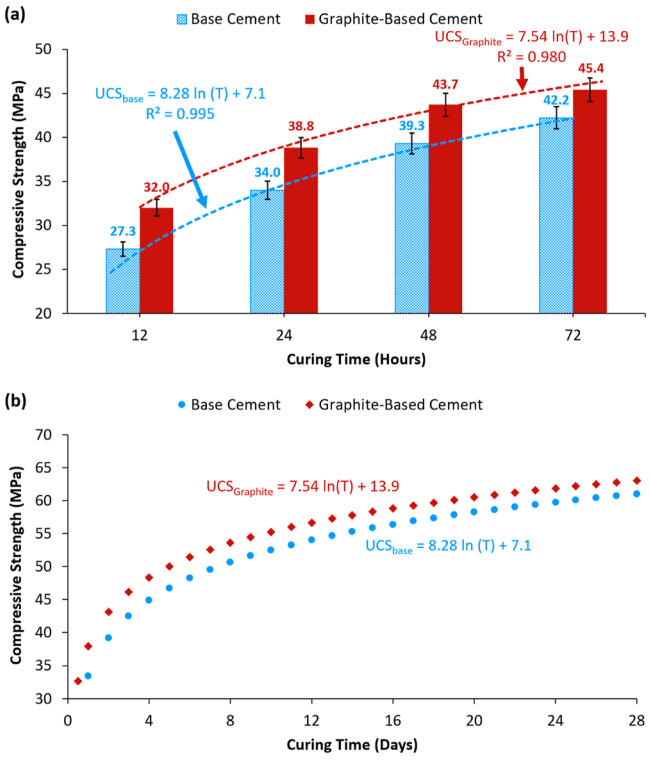

Figure 2. (a) Compressive strength after 12, 24, 48, and 72 h of curing for the base and graphite-based cement samples; (b) change of the cement compressive strength during 28 days.

$$\mathrm{UCS}_{\mathrm{base}} = 8.28 \ln(T) + 7.1 \quad (1)$$

$$\mathrm{UCS}_{\mathrm{Graphite}} = 7.54 \ln(T) + 13.9 \quad (2)$$

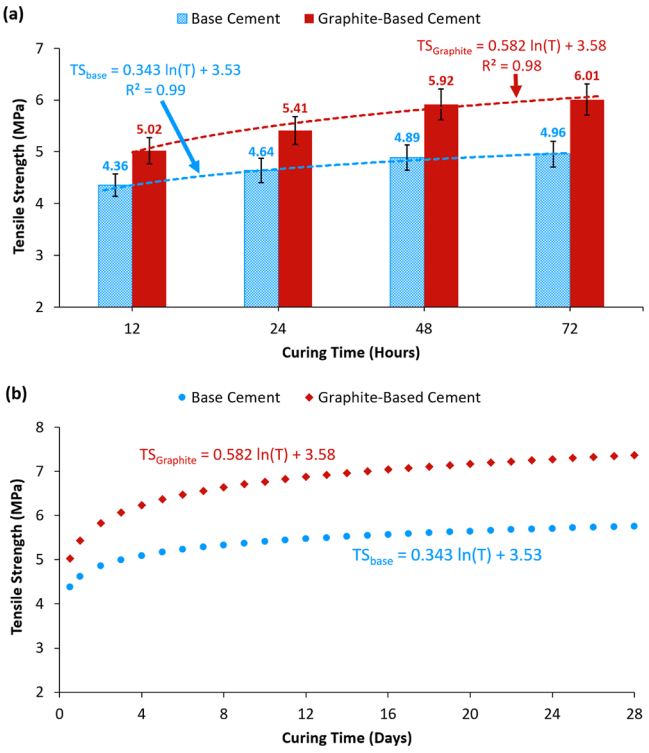

Figure 3. (a) Tensile strength after 12, 24, 48, and 72 h of curing for the base and graphite-based cement samples; (b) change of the cement tensile strength during 28 days.

where UCS is the unconfined compressive strength (MPa) and T is the curing time (days).

Relationships of the change of the compressive strength with curing time for both cementing systems were then derived based on the trends in Figure 2a. The equations of the trendline are shown in eqs 1 and 2. Using these equations, the compressive strength was predicted for both systems for the first 28 days of curing, as shown in Figure 2b.

The change in tensile strength is shown in Figure 3. Figure 3a shows the variation in the tensile strength with the curing time for the first three days of curing. As shown in this figure, graphite has a positive impact on tensile strength. After 12 h of curing, for example, the tensile strength of the base cement is 4.36 MPa, while graphite-based cement has a higher tensile strength of 5.02 MPa. 72 h after being cured, the base and graphite-based samples have a tensile strength of 4.96 and 6.01 MPa. Tensile strength indicates the resistance of the cement sheath to break under bending forces. With higher tensile strength, it shows that graphite can build a cement sheath that is more resistant to stretches and bending forces.

$$\mathrm{TS}_{\mathrm{base}} = 0.343 \ln(T) + 3.53 \quad (3)$$

$$\mathrm{TS}_{\mathrm{Graphite}} = 0.582 \ln(T) + 3.58 \quad (4)$$

where TS is the tensile strength (MPa).

Empirical equations representing the variation in tensile strength with time were developed based on matching of the variation during the first three days of curing; these equations are eqs 3 and 4. Using these equations, the tensile strength was predicted for the first 28 days of curing and is shown in Figure 3b. The graphs in Figure 3b show that the tensile strength of the cement will be increased faster in the first week period of time for both cement systems. Graphite also gave a positive impact where

https://doi.org/10.1021/acsomega.2c08253
ACS Omega 2023, 8, 8773−8778

the cement sheath strengthened faster with higher strength than the base cement core.

3.2. Poisson's Ratio and Young's Modulus. Poisson's ratio of both cement systems was evaluated, and the results are shown in Figure 4. As indicated in Figure 4a, Poisson's ratio of

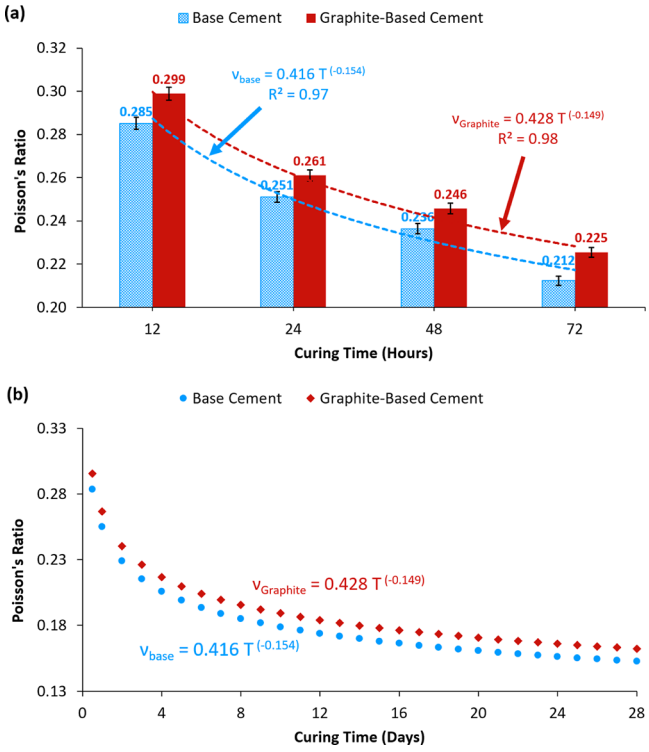

Figure 4. (a) Poisson's ratio after 12, 24, 48, and 72 h of curing for the base and graphite-based cement samples; (b) change of the Poisson's ratio during 28 days.

both systems was decreasing with curing time throughout the first three days; graphite tends to increase the Poisson's ratio of the hardened cement compared with that of base cement. The graphite has successfully increased the Poisson's ratio up to 104% within 48 and 72 h of curing. The highest difference is in 48 h of curing time, which reaches up to 0.02. A higher Poisson's ratio indicates that the cement is not easier to expand and incompressible, which is more desirable for the oil and gas well condition.[28]

$$v_{base} = 0.416\ T^{-0.154} \quad (5)$$

$$v_{Graphite} = 0.428\ T^{-0.149} \quad (6)$$

where v is the Poisson's ratio.

The equations representing the change in Poisson's ratio with curing time were derived from the best matching with the change in curing time during the first 3 days as indicated in Figure 4b; these equations are shown in eqs 5 and 6. Using these equations, the Poisson's ratio was predicted for the first 28 days of curing, as shown in Figure 4b. The graph shows a negative exponential trendline of Poisson's ratio with curing time; this figure also shows that Poisson's ratio decreases faster in the first week of the curing. Graphite also gave a positive impact where the cement system incorporating graphite has a higher Poisson's ratio, an average of 5% higher, compared to the base cement samples.

The alteration of Young's modulus with curing time is summarized in Figure 5. Figure 5a shows the variation of

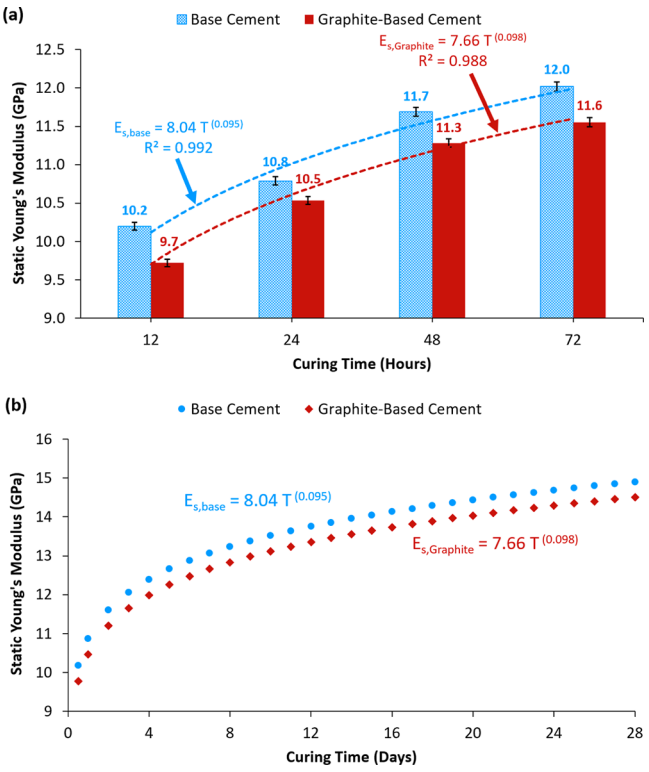

Figure 5. (a) Young's modulus after 12, 24, 48, and 72 h of curing for the base and graphite-based cement samples; (b) change of Young's modulus during 28 days.

Young's modulus for the first three days of curing. As indicated in this figure, Young's modulus decreases with the curing time for both cement systems, Young's modulus for the graphite-based cement is less than that for base cement throughout the curing time. After 12 h of curing, the base cement Young's modulus was 10.2 GPa which was then increased to reach 12.0 GPa after three days of curing. For the graphite-based samples, Young's modulus at 12 and 72 h were 9.7 and 11.6 Gpa, respectively. Young's modulus reflects the resistance of the cement sheath to deformation, especially under shear forces. The cement system with lower Young's modulus is more stable and has more ability to resist deformation caused by shear stresses.[29]

$$E_{s,base} = 8.04\ T^{0.095} \quad (7)$$

$$E_{s,Graphite} = 7.66\ T^{0.098} \quad (8)$$

where E_s is Young's modulus (GPa).

The trendline for the best fit of the change in Young's modulus during the first three days of curing was considered to extract equations representing the alteration of Young's modulus for the base and graphite-based cement, eqs 7 and 8, respectively. Using these equations, Young's modulus was predicted for the first 4 weeks of curing, as shown in Figure 5b. The graph shows a positive exponential trendline for Young's modulus with a faster increase in the first week of the curing. Graphite also gave a positive impact where the cement samples incorporating graphite have lower Young's modulus.

https://doi.org/10.1021/acsomega.2c08253
ACS Omega 2023, 8, 8773−8778

3.3. Porosity and Permeability.

Figure 6 shows the variation in porosity of both cement systems with curing time,

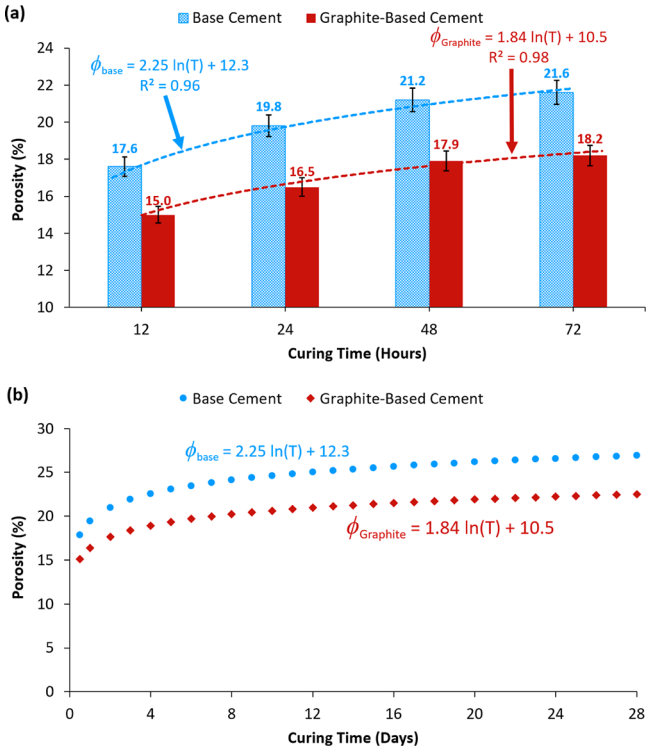

Figure 6. (a) Porosity after 12, 24, 48, and 72 h of curing for the base and graphite-based cement samples; (b) change of the porosity during 28 days.

for three days of curing (Figure 6a), and for 28 days of curing (Figure 6b). As shown in Figure 6a, the porosity of both systems was increasing with curing time, and the rate of increase in porosity was less during the early curing time; this is because of the dehydration process of the cement. Early dehydration could cause premature hardening.[30] With curing time, more water gets dehydrated and tends to form a tiny pore in the solids. For the base cement, the porosity increased from 17.6% after 12 h of hydration to 21.6% after 72 h. The porosity of graphite-based cement was lower than the base cement during the curing time; lowering the porosity means lesser pores in the solid, which indicates a more densified cement sheath. The porosity of graphite-based samples increased from 15.0 to 18.2% between 12 and 72 h of curing, respectively.

$$Ø_{base} = 2.25 \ln(T) + 12.3 \quad (9)$$

$$Ø_{Graphite} = 1.84 \ln(T) + 10.5 \quad (10)$$

where Ø is the porosity (%).

Relationships of porosity variation with curing time were derived for both cement systems, as shown by eqs 9 and 10. Using these equations, the porosity was predicted for the first 4 weeks of curing, as shown in Figure 6b. The graphs in Figure 6b show positive logarithmic trendlines of the porosity with a faster decrease in the first 3 days of the curing.

The permeability changes with curing time are summarized in Figure 7. Figure 7a summarized the variation in the first three days of curing. As shown in this figure, the permeability of both cement systems decreased with the curing time and the incorporation of graphite decreased the permeability of the

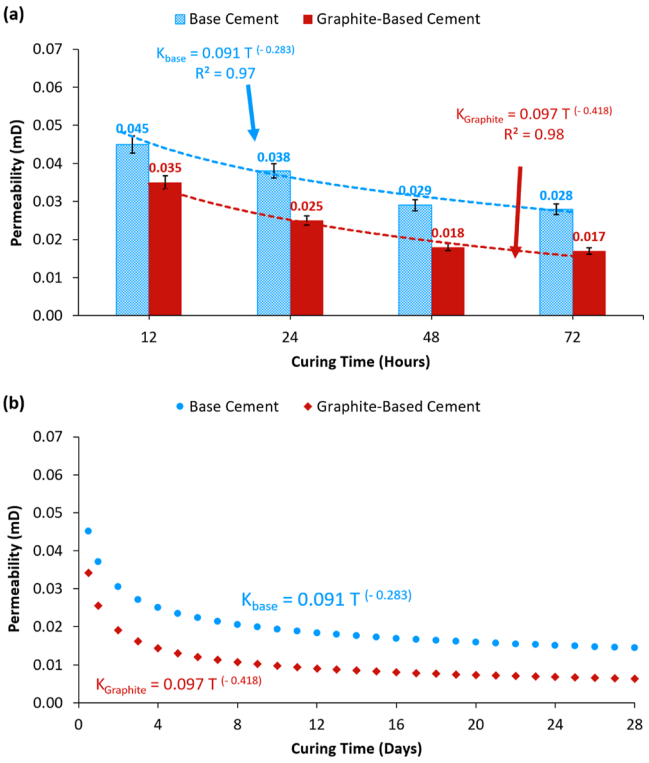

Figure 7. (a) Permeability after 12, 24, 48, and 72 h of curing for the base and graphite-based cement samples; (b) change of the permeability during 28 days.

cement. Lower permeability of the cement is important since it reduces the invasion of fluid into the cement sheath; therefore, it could increase the durability of the cement.

$$K_{base} = 0.091\ T^{-0.283} \quad (11)$$

$$K_{Graphite} = 0.097\ T^{-0.418} \quad (12)$$

where K is the permeability (mD).

Eqs 11 and 12 were extracted based on the best matching of the changes in permeability for both cement systems; these equations were used to find the permeability alteration during the first 28 days of curing with the results, as shown in Figure 7b. The graphs in Figure 7b show a negative logarithmic trendline of the permeability which decreased faster in the first week of the curing.

4. CONCLUSIONS

This study evaluates the effect of the graphite powder added to the cement slurry on the mechanical and elastic properties, porosity, and permeability of the hardened cement as a function of the curing time. The result can be summarized below.

- The incorporation of graphite increased the cement's sheath compressive and tensile strength.
- The cement sheath compressively was reduced by the incorporation of graphite into the cement slurry.
- The cement resistance to shear stresses was also improved by the incorporation of graphite as indicated by the decrease in the cement static Young's modulus.
- Incorporation of the graphite into the cement also leads to formation of the densified cement matrix as confirmed by the decrease in the porosity and permeability of the cement.

https://doi.org/10.1021/acsomega.2c08253
ACS Omega 2023, 8, 8773−8778

AUTHOR INFORMATION

Corresponding Author

Salaheldin Elkatatny − *College of Petroleum Engineering and Geosciences, King Fahd University of Petroleum & Minerals, Dhahran 31261, Saudi Arabia;* orcid.org/0000-0002-7209-3715; Email: elkatatny@kfupm.edu.sa

Authors

Muhammad Andiva Pratama − *College of Petroleum Engineering and Geosciences, King Fahd University of Petroleum & Minerals, Dhahran 31261, Saudi Arabia*

Ahmed Abdulhamid Mahmoud − *College of Petroleum Engineering and Geosciences, King Fahd University of Petroleum & Minerals, Dhahran 31261, Saudi Arabia*

Complete contact information is available at: https://pubs.acs.org/10.1021/acsomega.2c08253

Author Contributions

The manuscript was written by the contributions of all authors [M.A.P., S.E., and A.A.M.]. Authors have approved the final version of the manuscript.

Funding

This research received no external funding.

Notes

The authors declare no competing financial interest.

ACKNOWLEDGMENTS

The authors wish to acknowledge King Fahd University of Petroleum & Minerals (KFUPM) for permitting the publication of this work.

REFERENCES

(1) Lavrov, A.; Torsæter, M. Physics and Mechanics of Primary Well Cementing. *Physics and Mechanics of Primary Well Cementing*; Springer International Publishing, 2016.

(2) Mitchell, R. F.; Miska, S. Z. *Fundamentals of Drilling Engineering*; Society of Petroleum EngineersRichardson: Texas, USA, 2011.

(3) Ahmed, A.; Mahmoud, A. A.; Elkatatny, S. Development of Early Oil Well Cement Properties Using Laponite Particles *SPE Asia Pacific Drilling Technology Conference and Exhibition*; MS: Bangkok, Thailand, 2022; Vol. 9−10. Paper presented at the IADC/ August.

(4) Ahmed, A.; Mahmoud, A. A.; Elkatatny, S.; Al-Majed, A. Evaluation of Granite Waste and Silica Flour in Oil Well Cementing *Paper presented at the 55th U.S. Rock Mechanics/Geomechanics Symposium, Virtual* 2021.

(5) Ahmed, A.; Mahmoud, A. A.; Elkatatny, S.; Gajbhiye, R.; Majed, A. Application of Tire Waste Material to Enhance the Properties of Saudi Class G Oil Well Cement *Oil & Gas Show and Conference, event canceled*; Paper presented at the SPE Middle East, 2021November 2021. .

(6) Mahmoud, A. A.; Elkatatny, S. Improved durability of Saudi Class G oil-well cement sheath in CO2 rich environments using olive waste. *Construction and Building Materials* **2020**, *262*. DOI: 10.1016/j.conbuildmat.2020.120623.

(7) Ridha, S.; Yerikania, U. The Strength Compatibility of Nano-SiO2 Geopolymer cement for oil well under HPHT conditions. *J. Adv. Civ. Eng. Pract. Res.* **2015**, *5*, 6−10.

(8) Valliappan, A. K.; Suppiah, R. R.; Irawan, S.; Bayuaji, R. Development of New Green Cement for Oil Wells. *Mater. Sci. Forum* **2016**, *841*, 148−156.

(9) Davies, J. P.; Clarke, B. A.; Whiter, J. T.; Cunningham, R. J. Factors influencing the structural deterioration and collapse of rigid sewer pipes. *Urban Water* **2001**, *3*, 73−89.

(10) Kiran, R.; Teodoriu, C.; Dadmohammadi, Y.; Nygaard, R.; Wood, D.; Mokhtari, M.; Salehi, S. Identification and evaluation of well integrity and causes of failure of well integrity barriers (A review). *J. Nat. Gas Sci. Eng.* **2017**, *45*, 511−526.

(11) Dusseault, M. B.; Gray, M. N.; Nawrocki, P. A. *Why Oilwells Leak: Cement Behavior and Long-Term Consequences*: SPE-64733-MS, 2000.

(12) Chinzorigt, G.; Lim, M. K.; Yu, M.; Lee, H.; Enkbold, O.; Choi, D. Strength, shrinkage and creep and durability aspects of concrete including CO2 treated recycled fine aggregate. *Cem. Concr. Res.* **2020**, *136*, 106062.

(13) Wang, P.; Fu, H.; Guo, T.; Zuo, W.; Zhao, H.; Tian, L.; Chen, C. Volume deformation of steam-cured concrete with fly ash during and after steam curing. *Construction and Building Materials* **2021**, *306*, 124854.

(14) Broni-Bediako, E. Oil Well Cement Additives: A Review of the Common Types. *Oil & Gas Research* **2016**, *02*(). DOI: 10.4172/2472-0518.1000112.

(15) Suppiah, R. R.; Rahman, S. H. A.; Shafiq, N.; Irawan, S. Uniaxial compressive strength of geopolymer cement for oil well cement. *J. Pet. Explor. Prod. Technol.* **2020**, *10*, 67−70.

(16) Choolaei, M.; Rashidi, A. M.; Ardjmand, M.; Yadegari, A.; Soltanian, H. The effect of nanosilica on the physical properties of oil well cement. *Mater. Sci. Eng., A* **2012**, *538*, 288−294.

(17) Murtaza, M.; Rahman, M. K.; Al-Majed, A. A. *Effect of Nanoclay on Mechanical and Rheological Properties of Oil Well Cement Slurry Under HPHT Environment* International Petroleum Technology Conference Day 3 WedNovember 2016, Vol. *16*, 2016D031S047R003.

(18) Santra, A.; Boul, P. J.; Pang, X. Influence of Nanomaterials in Oilwell Cement Hydration and Mechanical Properties *Society of Petroleum Engineers - SPE International Oilfield Nanotechnology Conference 2012*; SPE-156937-MS, 2012.

(19) Ahmed, A.; Mahmoud, A. A.; Elkatatny, S.; Chen, W. The Effect of Weighting Materials on Oil-Well Cement Properties While Drilling Deep Wells. *Sustainability* **2019**, *11*, 6776.

(20) Ko, S.; Kwon, Y. J.; Lee, J. U.; Jeon, Y.-P. Preparation of synthetic graphite from waste PET plastic. *J. Ind. Eng. Chem.* **2020**, *83*, 449−458.

(21) Fuks, L.; Herdzik-Koniecko, I.; Kiegiel, K.; Zakrzewska-Koltuniewicz, G. Management of Radioactive Waste Containing Graphite: Overview of Methods. *Energies* **2020**, *13*, 4638.

(22) Cai, J.; Wang, M.; Zhou, S.; Cheng, X. Mechanical Properties of Graphite-Oil Well Cement Composites under High Temperature. *ACS Omega* **2022**, *7*, 14148−14159.

(23) Mahmoud, A. A.; Elkatatny, S.; Al-Majed, A.; Al Ramadan, M. The Use of Graphite to Improve the Stability of Saudi Class G Oil-Well Cement against the Carbonation Process. *ACS Omega* **2022**, *7*, 5764−5773.

(24) Balayssac, J. P.; Détriché, Ch. H.; Grandet, J. Effects of curing upon carbonation of concrete. *Construction and Building Materials* **1995**, *9*, 91−95.

(25) Kim, J.-K.; Moon, Y.-H.; Eo, S.-H. Compressive strength development of concrete with different curing time and temperature. *Cem. Concr. Res.* **1998**, *28*, 1761−1773.

(26) Nagral, M. R.; Ostwal, T.; Chitawadagi, M. V. Effect Of Curing Temperature And Curing Hours On The Properties Of Geo-Polymer Concrete *SP-179: Fourth CANMET/ACI/JCI Conference: Advances in Concrete Technology*. 2014; Vol. *12*.

(27) Mahmoud, A. A.; Elkatatny, S. The Effect of Silica Content on the Changes in the Mechanical Properties of Class G Cement at High Temperature from Slurry to Set *In the Proceedings of the 53rd US Rock Mechanics/Geomechanics Symposium held in New York*; Society of Petroleum Engineers: 23−26 June: USA, 2019.

(28) Ahmed, A.; Mahmoud, A. A.; Elkatatny, S. The Use of the Granite Waste Material as an Alternative for Silica Flour in Oil-Well Cementing. *ACS Omega* **2020**, *5*, 32341−32348.

(29) Ahmed, A.; Mahmoud, A. A.; Elkatatny, S.; Gajbhiye, R. Improving Saudi Class G Oil-Well Cement Properties Using the Tire Waste Material. *ACS Omega* **2020**, *5*, 27685−27691.

(30) Zhang, J.; Weissinger, E. A.; Peethamparan, S.; Scherer, G. W. Early hydration and setting of oil well cement. *Cem. Concr. Res.* **2010**, *40*, 1023−1033.